A&A 525, A148 (2011)
DOI: 10.1051/0004-6361/201014462
© ESO 2010

Astronomy & Astrophysics

Testing Newtonian gravity with distant globular clusters: NGC 1851 and NGC 1904⋆, ⋆⋆

R. Scarpa[1], G. Marconi[2], G. Carraro[2], R. Falomo[3], and S. Villanova[4]

[1] Instituto de Astrofísica de Canarias, Spain
e-mail: riccardo.scarpa@gtc.iac.es
[2] European Southern Observatory, Chile
[3] Osservatorio Astonomico di Padova, Italy
[4] Universidad de Concepcion, Departamento de Astronomia, Concepcion, Chile

Received 18 March 2010 / Accepted 19 August 2010

ABSTRACT

Context. Globular clusters are useful for testing the validity of Newtonian dynamics in the low acceleration regime typical of galaxies, without the complications of non-baryonic dark matter. In the absence of disturbing effects, such as tidal heating, the velocity dispersion of globular clusters is expected to vanish at large radii. If this is not observed, and in particular if, as observed in elliptical galaxies, the dispersion is found to be constant at large radii below a certain threshold acceleration, this might indicate a breakdown of Newtonian dynamics.

Aims. To minimize the effects of tidal heating that can increase the velocity dispersion at large radii, we study the velocity dispersion profile of two distant globular clusters, NGC 1851 and NGC 1904.

Methods. The velocity dispersion profile is derived from accurate radial velocity measurements, obtained at the ESO 8m VLT telescope with the FLAMES multi-object spectrograph. Reliable data for 184 and 146 bona fide cluster star members were obtained for NGC 1851 and NGC 1904, respectively.

Results. These data allow us to trace the velocity dispersion profile to $\sim 2r_0$, where r_0 is the radius at which the cluster internal acceleration of gravity is $a_0 \sim 10^{-8}$ cm s^{-2}. It is found that in both clusters the velocity dispersion is maximal at the center, decreases moving outward, and then becomes constant beyond $\sim r_0$. Since the distance of these clusters from the Milky Way is large, the observed flattening of the velocity dispersion profile cannot be ascribed to tidal heating effects, as proposed in the case of nearer globular clusters.

Conclusions. These results are in full agreement with those found for another five globular clusters previously investigated as part of this project. Taken together, our results for these 7 clusters support the claim that the velocity dispersion is constant beyond r_0, irrespectively of the specific physical properties of the clusters: mass, size, dynamical history, and distance from the Milky Way. The strong similarity to the constant velocity dispersion observed in elliptical galaxies beyond r_0 is indicative of a common origin for this phenomenon in the two class of objects, and possibly a breakdown of Newtonian dynamics below a_0.

Key words. gravitation – globular clusters: general

1. Introduction

Stars within galaxies, and galaxies within clusters of galaxies are very far apart from each other. As a consequence, the typical gravitational accelerations governing their dynamics are orders of magnitude smaller than those probed in our laboratories or in the solar system. Thus, any time Newton's law of gravity is applied to galaxies (e.g., to infer the existence of dark matter), its validity is severely extrapolated.

Although there are plenty of reasons to trust Newton's law in this very weak acceleration regime, it is well known that spiral galaxy rotation curves (see review by Sofue et al. 2001, and reference therein) systematically deviate from prediction of Newtonian dynamics. In a similar way elliptical galaxy (e.g., Carollo et al. 1995; Mehlert et al. 2000; Pu et al. 2010) and cluster of galaxy velocity dispersion profiles (e.g., Lokas et al. 2006), exibits a remarkable flattenings at large radii where a Keplerian falloff would be expected. These deviations, ascribed to the existence of large amounts of non-baryonic dark matter (DM), appears to exhibit systematic (but not yet understood) behaviors (cf., findings of Gentile et al. 2010; Donato et al. 2009). The most remarkable (e.g., Binney 2004) is that DM is needed to reconcile predictions with observations when and only when the acceleration of gravity goes below the *critical* value $a_0 \sim 10^{-8}$ cm s^{-2} (Begeman et al. 1991).

These results imply that we are witnessing a breakdown of Newton's law rather than the effects of DM. If this were the case, one should observe the same phenomenology in all systems where the acceleration decreases below a_0. In particular, the detection of a systematic flattening of the velocity dispersion profile in the external region of globular clusters, which are known to contain negligible quantities of DM, would represent a strong indication of a failure of the adopted law rather than the effects of unseen matter.

Scarpa et al. (2003) presented the results of a pilot study of the dynamics of the external region of the globular cluster ω Cen. The velocity dispersion was traced out to 45 pc from the center, probing acceleration as small as $\sim 7 \times 10^{-9}$ cm s^{-2}. Clear evidence was found that as soon as the internal acceleration of gravity approaches a_0, the velocity dispersion does not vanish,

⋆ Based on observations collected at the European Southern Observatory, Chile (Proposal 80.D-0106).
⋆⋆ Tables 2 and 3 are only available in electronic form at http://www.aanda.org

Table 1. NGC 1851 and NGC 1904 basic properties from Harris 1996.

NGC 1851		
RA, Dec (2000)	05:14:06.3 −40:02:50	Coordinates of cluster center
L, B	244.51 −35.04	Galactic coordinates
$R_{\rm sun}$	12.1 kpc	Distance from sun
$R_{\rm MW}$	16.7 kpc	Distance from Milky Way center
$V_{\rm los}$	320.5 km s^{-1}	Line of sight radial velocity
M_V	−8.33	Total V band magnitude
Mass/$M_\odot$	1.8×10^5	From luminosity assuming $M/L_V = 1$
$r_{\rm h}$	0.52 arcmin or 1.83 pc	Half light radius
$r_{\rm t}$	11.7 arcmin or 41.2 pc	Tidal radius
r_0	4.1 arcmin or 14.5 pc	Radius where $a = 1.2 \times 10^{-8}$ cm s^{-2}
Scale factor	3.52	pc/arcmin
NGC 1904		
RA, Dec (2000)	05:24:10.6 −24:31:27	Coordinates of cluster center
L, B	227.23 −29.53	Galactic coordinates
$R_{\rm sun}$	12.9 kpc	Distance from sun
$R_{\rm MW}$	18.8 kpc	Distance from Milky Way center
$V_{\rm los}$	206.0 km s^{-1}	Line of sight radial velocity
M_V	−7.86	Total V band magnitude
Mass/$M_\odot$	1.2×10^5	From luminosity assuming $M/L_V = 1$
$r_{\rm h}$	0.80 arcmin or 3.0 pc	Half light radius
$r_{\rm t}$	8.34 arcmin or 31.3 pc	Tidal radius
r_0	3.1 arcmin or 11.7 pc	Radius where $a = 1.2 \times 10^{-8}$ cm s^{-2}
Scale factor	3.75	pc/arcmin

converging toward a constant value. This claim was disputed by Sollima et al. (2009), but reconfirmed by Scarpa & Falomo (2010) by reanalyzing all available data.

This property of ω Cen is not unique and appears to occur in all globular clusters for which an adequate analysis of the velocity dispersion profile has been performed: NGC 6171 and NGC 7078 (Scarpa et al. 2004a,b), and NGC 7099 and NGC 6341 (Scarpa et al. 2007a,b).

The low concentration cluster NGC288 appears to be even more interesting. This cluster has internal accelerations of gravity every where below a_0 and thus is a tiny version of a low surface brightness spheroidal galaxy. As for galaxies (Mateo 1997; Wilkinson et al. 2006; Koch et al. 2007), NGC 288 has within its measurements errors the same velocity dispersion at all radii (Scarpa et al. 2007b). Another low-density cluster for which deviations from Newtonian dynamics are possible found is Palomar 14 (Gentile et al. 2010).

These results highlight an interesting correspondence between elliptical galaxies and globular clusters. Dense globular clusters have the same accelerations as and behave like high surface brightness elliptical galaxies, while loose clusters have the same accelerations as and behave like low surface brightness elliptical galaxies. What is different is the interpretation of the data. It is commonly accepted that in galaxies dark matter alters the dynamics, while in globular clusters something else does.

The most viable explanation for globular clusters appears to be tidal heating, the increase in the stellar velocity dispersion caused by the differential acceleration produced by the Milky Way in different position of the globular cluster. It would be, however, more logic to invoke a common origin of the phenomenon, that is a failure of Newtonian dynamics below a_0 as claimed within the framework of MOND (Milgrom 1983).

To generalize our investigation, we present new accurate radial velocity measurements for NGC 1851 and NGC 1904 (Table 1). These clusters were selected for being located at $r = 16.7$ and 18.8 kpc from the Galactic center, respectively, which is approximately twice as distant from the Milky Way center as the other globular clusters studied so far. Thus these clusters are experiencing a tidal heating, proportional to r^{-3}, about one order of magnitude smaller, making its effects negligible.

2. Observation and data analysis

The initial selection of targets was based on their color, as derived from the analysis of ESO Imaging Survey frames and ESO 2.2 m Wide Field Imager data. Targets were selected if their color difference from the cluster main sequence was $V-I < 0.05$ and $V - I < 0.1$, and apparent magnitude $19 > m > 18$ and $19 > m > 17$, for NGC 1851 and 1904, respectively. The cut in luminosity was made close to the base of the giant branch to probe the cluster stellar population in a well populated region to ensure a high probability of finding cluster members at large distances from the cluster. According to Milky Way stellar population models (Vanhollebeke et al. 2009) we expect a contamination of only 0.029 and 0.118 stars per arcmin squared in the selected color-luminosity range, corresponding to about 1.8% and 7.5% of our initial target list, for NGC 1851 and 1904, respectively.

In Figs. 1 and 2, we show the color-magnitude diagram (CMD) of the clusters highlighting the positions of the 199 and 173 stars that were actually observed in NGC 1851 and 1904, respectively. The final distribution of the targets around the cluster center is also shown.

Because of the moderately high Galactic latitude and the high quality photometric data, we did expect little contamination and a very high success rate in identifying cluster members.

Spectroscopic observations were obtained with FLAMES+GIRAFFE (Pasquini et al. 2002) at the ESO 8 meter VLT telescope. FLAMES is a fiber multi-object spectrograph, allowing the simultaneous observation of up to 130 objects. We selected the HR9B setup that includes the magnesium triplet covering the wavelength range 5143 Å $< \lambda <$ 5346 Å at resolution $R = 25\,900$. Stellar astrometry was derived using data from the US Naval Observatory (USNO) catalog, which proved to have the required accuracy (0.3 arcsec) for FLAMES observations. Two different fiber configurations were necessary to allocate all the selected stars. For each configuration five separate 3200 s exposures were obtained on different night from November 2007 to March 2008, under good atmospheric conditions (clear sky, airmass <1.5, and seeing ∼1 arcsec).

Data were automatically pre-reduced using the GIRAFFE pipeline GIRBLDRS[1], in which the spectra have been debiased, flat-field corrected, extracted, and wavelength-calibrated, using both prior and simultaneous calibration-lamp spectra. A sky correction was applied to each stellar spectrum by subtracting the average sky spectra obtained through dedicated fibers. The resulting spectra have a dispersion of 0.05 Å/pixel.

Radial velocities were obtained from the IRAF fxcor cross-correlation task. Stellar spectra were cross-correlated with a synthetic template calculated by SPECTRUM, the LTE spectral synthesis program freely distributed by Richard O. Gray[2], for the mean temperature, gravity $\log g$, and metallicity of our stars. We verified on the Kurucz solar flux atlas and UVES solar spectra that the template was accurate at the level of 50 m/s or less. The accuracy of the data reduction procedure and the radial velocity measurement was extensively tested in previous works (e.g. Milone et al. 2006; Sommariva et al. 2009).

[1] Blecha et al. (2000); see http://girbldrs.sourceforge.net for the GIRAFFE pipeline software and documentation

[2] Program and documentation available at www.phys.appstate.edu/spectrum/spectrum.html.

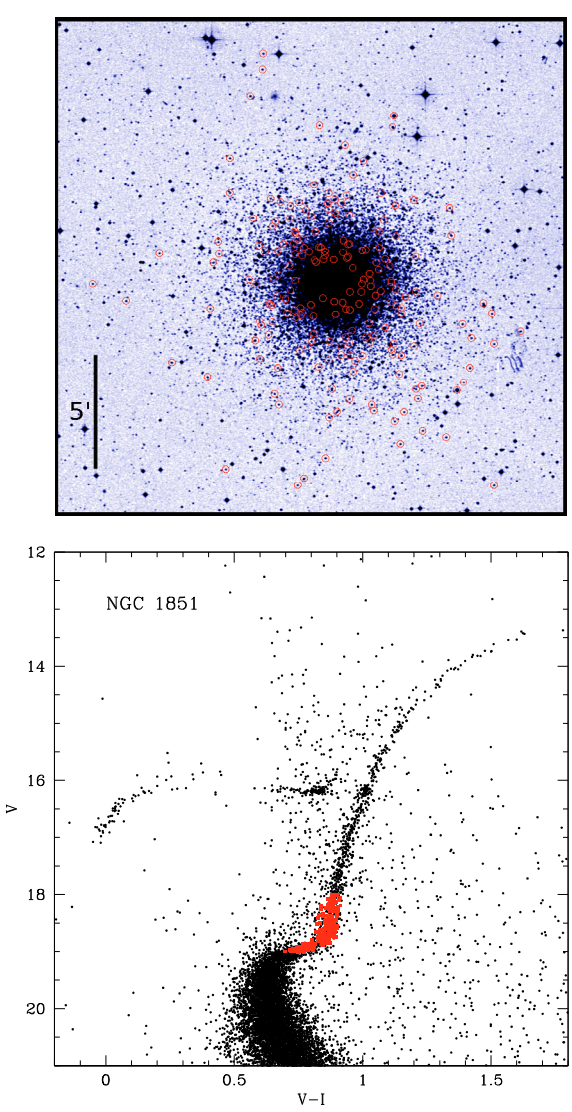

Fig. 1. The distribution of the selected stars in the cluster NGC1851 (north on *the top*, east on *the left*), and the color–magnitude diagram with the selected targets highlighted in red. For reference, the radius where the acceleration of gravity is a_0 is 2.9 arcmin.

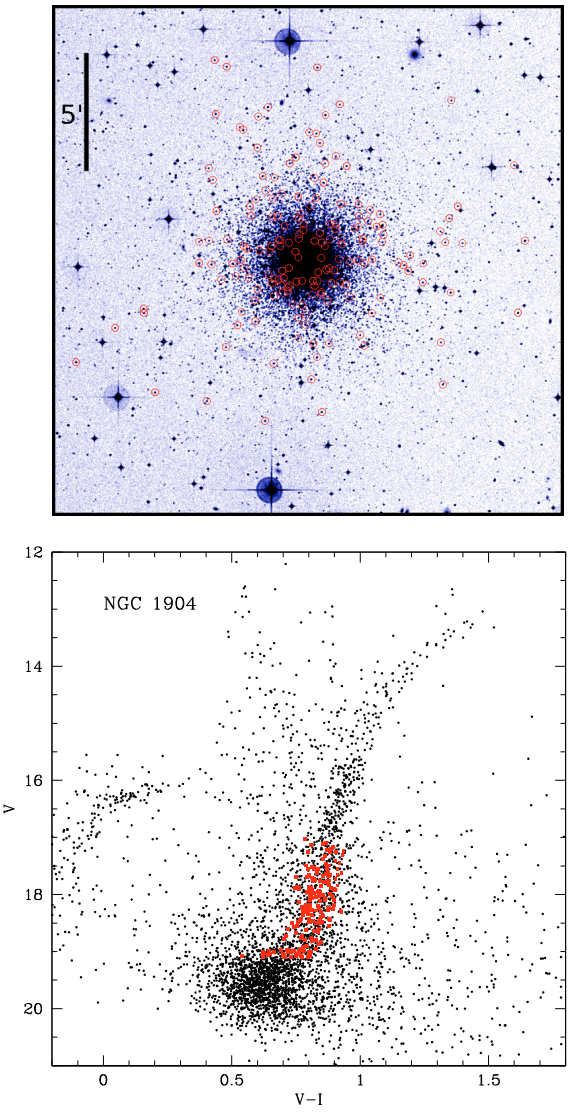

Fig. 2. The distribution of the selected stars in the cluster NGC 1904 (north on *the top*, east on *the left*), and the color-magnitude diagram with the selected targets highlighted in red. For reference, the radius where the internal acceleration of gravity is a_0 is 2.1 arcmin.

Each spectrum was treated independently from the others, so that we ended up with 5 independent measurements of the radial velocity for each star. For a limited number of stars, we have fewer than 5 spectra because some were rejected for being affected by strong cosmic rays and other defects. The exact number of spectra available for each star is given in Tables 2 and 3. These radial velocities were then used to determine the effects of any intrinsic variation in the radial velocity (e.g., due to binary stars, stellar photospheric winds, measurement errors, etc.) finding for the vast majority of the targets a dispersion of less than 2.0 and 1.5 km s^{-1} in the case of NGC 1851 and NGC 1904, respectively (Fig. 3). This corresponds to a statistical uncertainty of less than 1 km s^{-1} in the average radial velocity of each target, small enough to not affect the measurement of the velocity dispersion of the cluster even in the most external regions. In the following, we define our most reliable estimate of the true radial velocity to be the weighted average of the 5 independent measurements.

A number of stars (5 in NGC 1851 and 8 in NGC 1904) were included in both FLAMES fiber setup to double check whether a velocity shift could exists between the two data sets. No statistically significant shift was detected down to 100 m/s. All velocities presented here are heliocentric.

3. Results

To derive the velocity dispersion profile (VDP), we first separated members from non-members in the velocity space. There was little ambiguity because the distribution of radial velocities was found to be bimodal, with separation of ∼100 km s^{-1}. In total, 4 non-members (2% of the sample) were found in NGC 1851 and 14 (8% of the sample) in NGC 1904, confirming a posteriori the high efficiency of our color selection criteria and in agreement with the expectations of galaxy stellar population models (see Sect. 2).

The median of the radial velocity error distribution for all members is 0.43 and 0.29 km s^{-1} (Fig. 3), significantly smaller than the expected velocity dispersion we are trying to measure (see next section). The radial velocity errors for a small fraction of the targets deviate significantly from those of the rest of the distribution. Thus we decided to retain only measurements

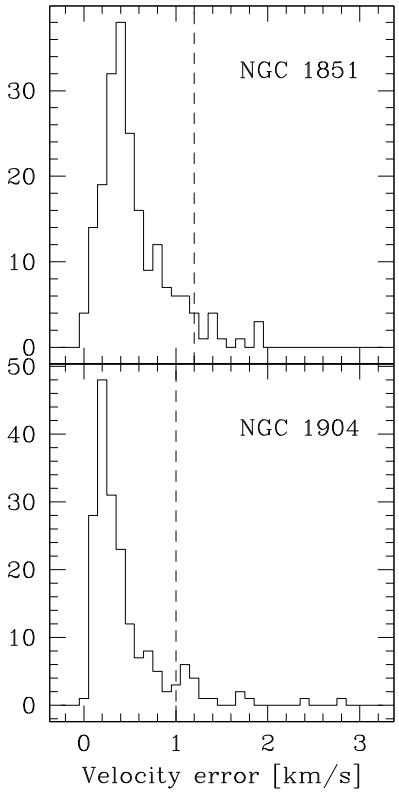

Fig. 3. Distribution of velocity uncertainties derived from the comparison of repeated velocities measurements of the same target. The peak of the distribution is at ∼0.4 and ∼0.2 km s^{-1} in NGC 1841 and 1904, respectively. This difference is due to targets in NGC 1904 being on average 0.4 mag brighter than those in NGC 1851. The dashed vertical line is the adopted threshold for rejecting objects.

with errors smaller than four times the semi-interquartile range of the error distribution (i.e., 1.2 and 1.0 km s^{-1} for NGC 1851 and 1904).

3.1. NGC 1851

From the initial sample of 199 stars, after eliminating 4 non-members cutting on radial velocity, and retaining only stars with a velocity accuracy higher than 1.2 km s^{-1} , we are left with 184 reliable radial velocities that represent the final sample used to constrain the cluster dynamics. The cluster average radial velocity is 320.0 ± 0.4 km s^{-1}, with rms of 4.9 km s^{-1}, in good agreement with the value 320.5 ± 0.6 km s^{-1} (Harris 1996). The average radial velocity within each bin shows no systematic trends as a function of distance from the cluster center (Fig. 4).

The cluster is slowly rotating, with a maximum ordered rotation velocity of less than 0.8 km s^{-1}, in both the inner and external regions (Fig. 5). Such a small rotational velocity cannot contribute significantly to support the structure of the cluster and is therefore neglected in the following discussion.

The velocity dispersion was computed in a number of selected bins following the procedure described in (Scarpa & Falomo 2010). Since the shape of the VDP might depend on the choice of the binning, we investigated the effects of different binning on the VDP. Two representative cases are shown. The first (Fig. 6) was obtained grouping the data using integer numbers in radial distance. The binning limits, the number of objects in each bin, and the corresponding velocity dispersion are given in Table 4. In the second case (Fig. 7), data were grouped by assigning a fixed number of objects to each bin, 20 in this case,

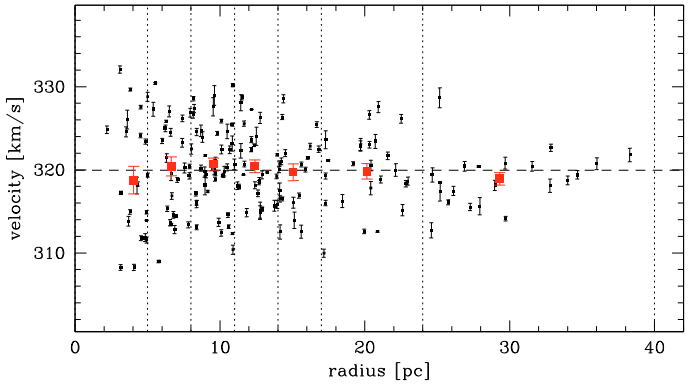

Fig. 4. The distribution of the 184 targets with radial-velocity uncertainty <1.2 km s^{-1} as a function of distance from the center of NGC 1851 (Points with error bar). The large squares with error bar represent the average velocity in the bins indicated by vertical lines. The horizontal dashed line represents the cluster mean radial velocity.

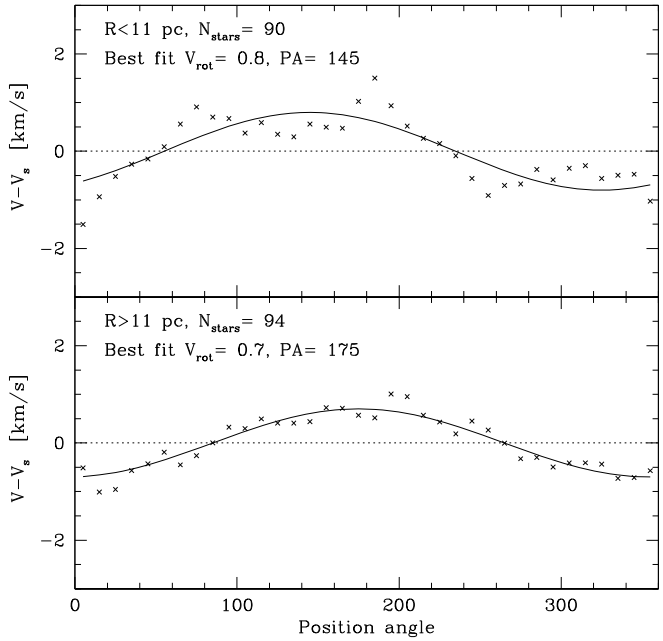

Fig. 5. Rotation in the inner and outer regions of NGC 1851. The plotted value is the average radial velocity of stars in a 180 degree sector, minus the average velocity of the whole cluster. The half cluster sector has been moved by 10 degrees from one point to the next. The maximum rotational velocity in km s^{-1} is derived from the best sinusoidal fit of the data. The position angle (in degrees from North toward East) of the rotation axis is also shown.

and moving by 5 objects from one bin to the next. This ensures a much higher sampling of the profile, because data are partially reused moving from one bin to the other, at the expenses of having statistically correlated values. While it is clear that because of the limited amount of data the velocity dispersion fluctuates quite significantly, the general trend is well defined. Toward the center, the velocity dispersion naturally extrapolates to the central velocity dispersion available in the literature (10.4 km s^{-1}, Harris 1996). In the external regions, the dispersions flattens out converging toward a constant value of ∼4.0 ± 0.5 km s^{-1}. Moving from the center outward, the VDP exhibits fluctuations of up to ∼2 km s^{-1}, making it difficult to identify the radius at which the flattening first occurs. This can be as close as 10 arcmin from the center, or as far as 15 arcmin. Assuming M/L = 1 in solar units,

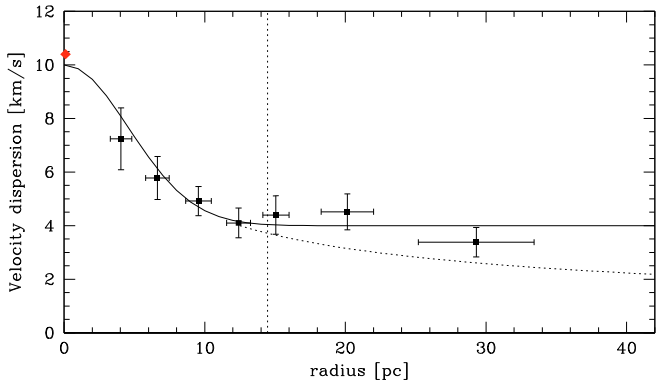

Fig. 6. NGC 1851 velocity dispersion computed binning the data as in Fig. 4. Error bars along the X axis represent the dispersion of the data within the bin; along the Y axis they give the 1-σ uncertainty in the dispersion. The central velocity dispersion as given in Harris (1996) is also shown (diamond). The vertical line marks the radius where the acceleration is a_0. Overplotted on the data is a Gaussian plus a constant, which is not a fit to the data, but is meant to highlight the flattening of the velocity dispersion that occurs well within the cluster tidal radius of 41 pc (Harris 1996). The dotted line falls as $r^{-1/2}$.

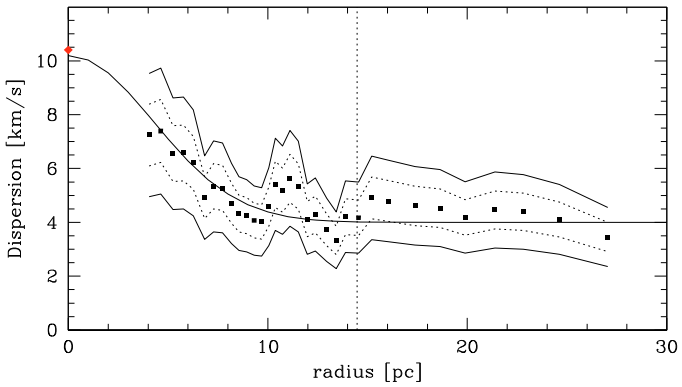

Fig. 7. The velocity dispersion profile of NGC 1851, derived considering the 184 members with radial velocity accuracy better than 1.2 km s^{-1}. Data have been binned in groups of 20 each, moving by 5 from one group to the next. The dotted and solid lines give the 66 and 90 percent confidence regions for the dispersion. The central velocity dispersion as reported in Harris (1996) is also shown (diamond). The vertical line marks the radius where the internal acceleration of gravity is a_0 (assuming $M/L = 1$). Overplotted on the data is a Gaussian plus a constant (not a fit to the data) to highlight the flattening of the VDP that occurs well within the cluster tidal radius of 41 pc (Harris 1996).

Table 4. Radial velocity dispersion for NGC 1851.

Bin [pc]	N stars	Bin center	σ [km s^{-1}]
0–5	20	4.05 ± 0.77	7.24 ± 1.16
5–8	27	6.64 ± 0.84	5.78 ± 0.80
8–11	43	9.55 ± 0.91	4.92 ± 0.54
11–14	29	12.40 ± 0.85	4.10 ± 0.56
14–17	20	15.05 ± 0.93	4.40 ± 0.72
17–24	24	20.14 ± 1.87	4.52 ± 0.67
24–40	21	29.30 ± 4.12	3.38 ± 0.55

a total V-band absolute magnitude for the cluster of $M = -8.33$, and distance from the Sun 12.1 kpc (Harris 1996), the internal acceleration of gravity is a_0 at $r = 14.5$ pc from the center. Thus, data are consistent with a flattening of the dispersion profile where $a < a_0$.

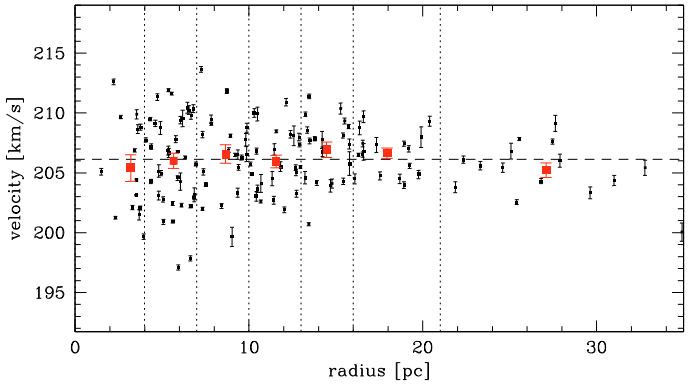

Fig. 8. The radial velocity distribution of the 146 targets with radial-velocity accuracy higher than 1.0 km s^{-1} (dots) as a function of distance in parsecs from the center of NGC 1904. The squares with error bars represent the average velocity in each bin indicated by the vertical lines. The horizontal dashed line indicates the cluster mean radial velocity.

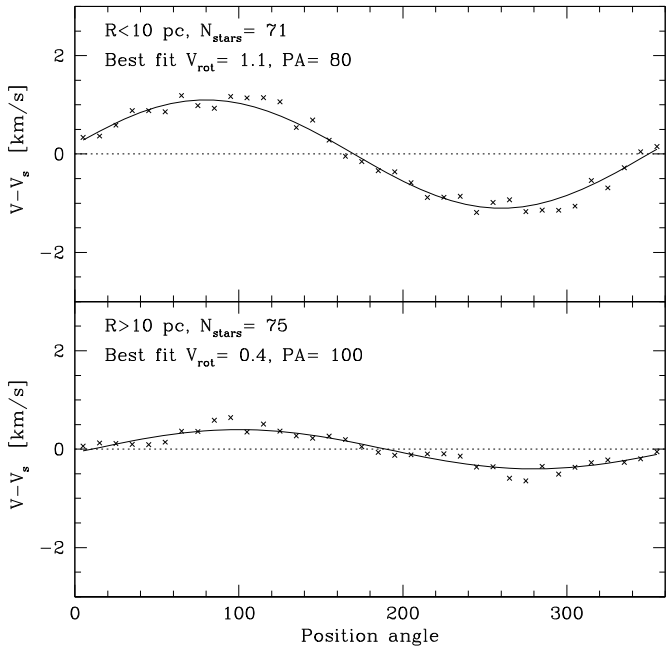

Fig. 9. Rotation in the inner and outer regions of NGC 1904. The plotted values represent the difference between the average radial velocity of stars in a 180 degree sector and the systemic velocity of the whole cluster. The maximum rotational velocity in km s^{-1} is derived from the best sinusoidal fit of the data. The position angle (in degrees from North toward East) of the rotation axis is also shown.

3.2. NGC 1904

From the initial sample of 173 stars, the cut on radial velocity and a velocity accuracy higher than 1.0 km s^{-1} left us with 146 targets used to study the cluster dynamics. The average radial velocity of NGC 1904 is 206.1 ± 0.3 km, with an rms of 3.1 km s^{-1}, in good agreement with the value available in the literature (206 ± 0.4, Harris 1996). No systematic trend is seen in the average radial-velocity distribution as a function of distance from the cluster center (Fig. 8).

The cluster is slowly rotating (Fig. 9). Within 3 arcmin from the center, we measured a rotation velocity of 1.1 km s^{-1}, at a position angle 85 degrees (from North toward East). At larger radii, the best sinusoidal fit is consistent with no rotation at all.

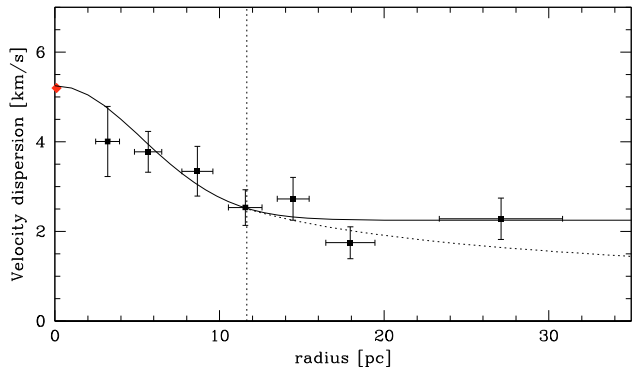

Fig. 10. The velocity dispersion of NGC 1904 computed with the same binning used in Fig. 8. Error bars along the x axis represent the dispersion of the data within each bin, along the y axis they give the 1-sigma uncertainty in the dispersion. The central velocity dispersion as given in Harris (1996) is also shown (diamond). The vertical dotted line marks the radius where the acceleration is a_0. Overplotted on the data is a Gaussian plus a constant, not a fit to the data, meant to highlight the flattening of the velocity dispersion that occurs well within the cluster tidal radius of 31 pc (Harris 1996). The dotted line falls as $r^{-1/2}$.

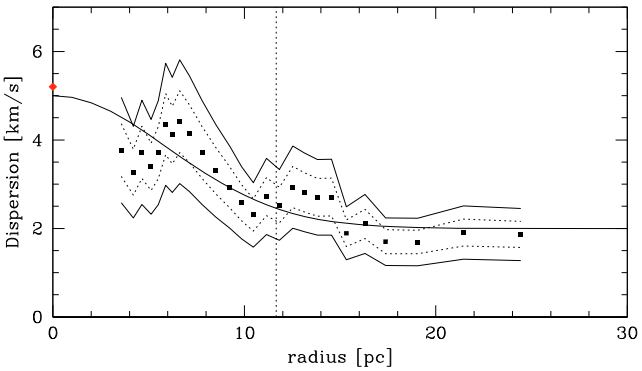

Fig. 11. Velocity dispersion profile of NGC 1904 as derived binning data in groups of 20 each, moving by 5 from one group to the next. The dotted and solid lines give the 66 and 90 percent confidence regions for the dispersion. The central velocity dispersion as reported in Harris (1996) is also shown (diamond). The vertical line indicates the radius where the internal acceleration of gravity is a_0 (assuming $M/L = 1$). Overplotted on the data is a Gaussian plus a constant, not a fit to the data, used to highlight the flattening of the VDP that occurs well within the cluster tidal radius of 31 pc (Harris 1996).

We can therefore neglect rotation in the outer part of the cluster, the most relevant to this study.

As for NGC 1851, we present the VDP derived with two different binning approaches (See Table 5, Figs. 10 and 11). Because of the low mass of NGC 1904 cluster, the dispersion is quite small and it is difficult with the present data set to derive a compelling result. All binning approaches used, however, appear to show that toward the center the profile might be consistent with a central velocity dispersion of 5.2 km s^{-1} reported in the literature (Harris 1996), Moving outward, the dispersion both increases and decreases a couple of times before converging toward a constant value of 2.25 ± 0.3 km s^{-1}. Starting from 10 pc away from the center, the dispersion varies within the range $1.8 < \sigma < 2.6$ km s^{-1}.

Assuming $M/L = 1$ in solar units, a total V-band absolute magnitude for the cluster of $M = -7.86$, and distance from the Sun 12.9 kpc (Harris 1996), the internal acceleration of gravity is a_0 at $r = 11.6$ pc from the center. Thus, also in this cluster data suggest a flattening of the VDP might occur at this particular value of the acceleration.

Table 5. Radial velocity dispersion for NGC 1904.

Bin [pc]	N stars	Bin center	σ [km s^{-1}]
0–4	14	3.20 ± 0.73	4.01 ± 0.78
4–7	37	5.66 ± 0.83	3.78 ± 0.46
7–10	20	8.65 ± 0.95	3.34 ± 0.55
10–13	24	11.56 ± 1.02	2.53 ± 0.40
13–16	19	14.47 ± 0.97	2.73 ± 0.48
16–21	17	17.94 ± 1.49	1.75 ± 0.35
21–35	15	27.09 ± 3.74	2.28 ± 0.46

4. Discussion

We have reported radial velocity measurements for two moderately distant globular clusters, NGC 1851 and 1904, located at 16.7 and 18.8 kpc from the Galactic center, respectively. The analysis of these data indicates that in these clusters the velocity dispersion remains constant beyond $r = 12.5 \pm 2.5$ and $r = 12 \pm 2$ pc from the center, respectively. These values are very similar to and statistically fully consistent with the radius r_0 where the acceleration is a_0.

Moreover, the two clusters are moving in a rapidly receding orbit. Assuming a logarithmic gravitational potential for the Milky Way, Dinescu et al. (1999) computed the most probable orbits of both NGC 1851 and NGC 1904. Integration of these orbits shows that they passed perigalacticon about 51 and 86 Myr ago, respectively. According to our velocity dispersion measurements, even in the outermost regions of the clusters the stellar velocity dispersion is 3.4 and 2.3 km s^{-1}. With this velocity dispersion, stars in NGC 1851 and NGC 1904 cover a distance of twice the tidal radius in ∼24 and ∼32 Myr, respectively, less than the time since last perigalacticon. Hence these clusters had enough time to revirialise. Moreover, these two clusters experience a tidal action due to the Milky Way about one order of magnitude smaller than that acting on the clusters previously studied as part of this project, making it unlikely that the flattening of the VDP is the result of tidal heating.

Thus, these new observations bring to 7 out of 7 the number of high concentration globular clusters showing constant velocity dispersion at large radii (Table 6).

While differing in many respects (mass, dynamical history, concentration, position in the Milky Way halo, etc.), these clusters do share the property of being sufficiently concentrated to have internal accelerations of gravity above a_0 at their centers, and thus behave in a asimilar way to high surface brightness elliptical galaxies (e.g., Carollo et al. 1995; Mehlert et al. 2000).

The available velocity dispersion data, however, in no case probe radii larger than $2.5r_0$. At this radius the hypothesis that the velocity dispersion is constant, predicts a dispersion 60% higher than what Newtonian dynamics predicts, assuming the two coincide at r_0. This difference is small enough that taken singularly none of these clusters represents a compelling case in favor (or against) a Keplerian falloff of the velocity dispersion. Therefore Newtonian dynamics remains a viable explanation to describe the data of individual objects (e.g., Moffat & Toth 2008). To increase the strength of the signal, we then combine the VDP of all the clusters. Data are normalized by plotting distance in units of r_0, and dispersions in units of σ_0, the dispersion at r_0. We note that compared to the full cluster size, r_0 corresponds to a very large radius, within which virtually all the cluster mass is contained. Thus, regardless of the exact mass distribution within the clusters, for $r > r_0$ the dispersion should follow closely a Keplerian decline (unless external effects alters it).

Table 6. Clusters with velocity dispersion data probing accelerations below a_0.

Name	$R_\odot$ [kpc]	R_{MW} [kpc]	M(v)	Mass [$M_\odot$]	r_0 [pc]	r_{tidal} [pc]	r_{flat} [pc]	σ [km s^{-1}]	a @ r_{flat} [10^{-8} cm s^{-2}]
NGC 1851	12.1	16.7	−8.33	1.8×10^5	14.5	41	12.5 ± 2.5	4.0 ± 0.5	1.6 ± 0.4
NGC 1904 (M79)	12.9	18.8	−7.86	1.2×10^5	11.7	31	12 ± 2	2.25 ± 0.4	1.1 ± 0.3
NGC 5139 (ω Cen)	5.5	6.4	−10.29	1.1×10^6	35.7	72	32 ± 3	7 ± 1	1.5 ± 0.4
NGC 6171 (M107)	6.4	3.3	−7.13	5.9×10^4	8.0	32	8 ± 2	2.7 ± 0.3	1.3 ± 0.6
NGC 6341 (M92)	8.2	9.6	−8.20	1.6×10^5	13.6	36	12 ± 2	3.1 ± 0.4	1.5 ± 0.6
NGC 7078 (M15)	10.3	10.4	−9.17	3.9×10^5	21.3	64	20 ± 2	3.2 ± 0.5	1.4 ± 0.4
NGC 7099 (M30)	8.0	7.1	−7.43	7.8×10^4	9.6	43	10 ± 2	2.2 ± 0.3	1.1 ± 0.4

Notes. The meaning of the columns is as follows. 1) Cluster name; 2) distance of the clusters from the sun; 3) distance from Milky Way center; 4) absolute total V band magnitude, used to derive the mass assuming $M/L = 1$ in solar units; 5) cluster mass from luminosity in solar masses; 6) radius where the acceleration is $a_0 = 1.2 \times 10^{-8}$ cm s^{-2}; 7) cluster tidal radius from Harris 1996; 8) radius where the velocity dispersion profile flattens out; 9) cluster asymptotic velocity dispersion; 10) acceleration at the radius r_{flat}.

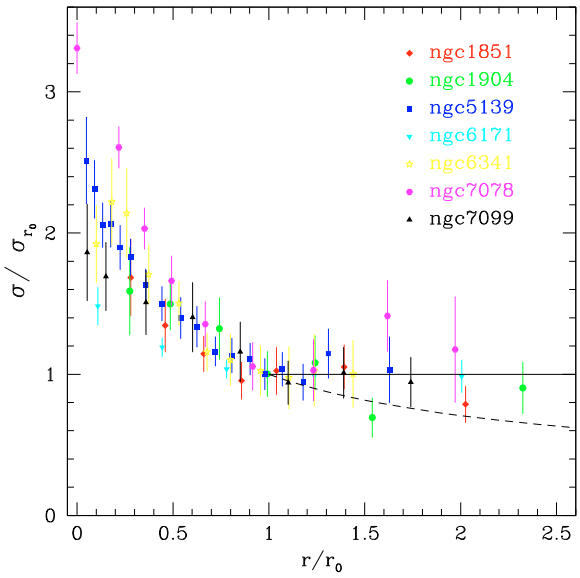

Fig. 12. Normalized velocity dispersion profile for all high density clusters studied so far as part of this program. Radii are in units of r_0, the radius where the acceleration is a_0, computed assuming $M/L = 1$ for all clusters. The dispersion is normalized to the value at r_0 to ensure in the region $r > r_0$ profiles from different clusters are comparable. The solid line at $d = 1$ represent a constant velocity dispersion, while the dashed line gives the Keplerian falloff. Data for NGC 1851 and NGC 1904 are from this work, for NGC 5139 from Scarpa & Falomo (2010), for NGC 6171 from Scarpa et al. (2004a,b), and for NGC 7099 and NGC 6343 from Scarpa et al. (2007a).

The systematic deviation of the VDP from the Newtonian prediction is now more evident, for all the points but one are above the Keplerian falloff (Fig. 12). To quantify the difference between the two models, we first notice that they must coincide for $r = r_0$. Therefore we limit the comparison to the 16 points at $r > 1.2r_0$. The hypothesis $\sigma/\sigma_0 = 1$ is statistically acceptable ($\chi^2 = 12.0$ for 15 degrees of freedom, probability 67%), while a curve falling as $x^{-1/2}$ has $\chi^2 = 26.9$ and can be rejected at the 97% confidence level.

The comparison of a K-S test between the observed data and the theoretical models show the constant dispersion hypothesis is about 15 times more probable then the Keplerian falloff.

The main conclusion of our work is that all globular clusters exhibit a flattening of the VDP at large radii. The explanation for this phenomenon cannot be the tidal action of the Milky Way, but has to be something else that applies to all clusters, independently of their location in the Milky Way halo.

This picture would be in good agreement with the prediction of the MOND hypothesis, in the case of no strong gravitational external field (Milgrom 1983). However, according to the MOND original formulation in none of these clusters we should observe deviations from Newtonian dynamics, because the external field of the Milky Way is close to or above a_0. Therefore, our results appear formally in disagreement with MOND predictions.

Acknowledgements. We thank Y. Momany for providing the photometry of NGC 1851, D. Bettoni for useful comments, and the Italian Space Agency for economical support by ASI-COFIC contract n. I/016/07/0 “Studi di Cosmologia e Fisica Fondamentale”.

References

Begeman, K. G., Broeils, A. H., & Sanders, R. H. 1991, MNRAS, 249, 523
Binney, J. 2004, in Dark Matter in Galaxies, ed. S. D. Ryder, D. J. Pisano, M. A. Walker, & K. C. Freeman, IAUS, 220, 3
Carollo, C. M., de Zeeuw, P. T., van der Marel, R. P., Danziger, I. J., & Qian, E. E. 1995, ApJ, 441, L25
Donato, F., Gentile, G., Salucci, P., et al. 2009, MNRAS, 397, 1169
Gentile, G., Famaey, B., Angus, G., & Kroupa, P. 2010, A&A, 509, A97
Harris, W. E. 1996, AJ, 112, 1487
Koch, A., Kleyna, J. T., Wilkinson, M. I., et al. 2007, ApJ, 134, 566
Lokas, E. L., Wojtak, R., Gottlöber, S., Mamon, G. A., & Prada, F. 2006, MNRAS, 367, 1463
Mateo M. 1997, on The nature of Elliptical Galaxies, ed. M. Arnaboldi, ASPC, 116, 259
Mehlert, D., Saglia, R. P., Bender, R., & Wegner, G. 2000, A&AS, 141, 449
Milgrom, M. 1983, ApJ, 270, 365
Milone, A. P., Villanova, S., Bedin, L. R., et al. 2006, A&A, 456, 517
Moffat, J. W., & Toth, V. T. 2008, ApJ, 680, 1158
Pasquini, L., Avila, G., Blecha, A., et al. 2002, The Messenger, 110, 1
Pu, S. B., Saglia, R. P., Fabricius, M. H., et al. 2010, A&A, 516, A4
Sollima, A., Bellazini, M., Smart, R. L., et al. 2009, MNRAS, 396, 2183
Scarpa, R., & Falomo, R. 2010, MNRAS, in press
Scarpa, R., Marconi, G., & Gilmozzi, R. 2003, A&A, 405, L15
Scarpa, R., Marconi, G., & Gilmozzi, R. 2004a, IAUS, 220, 215
Scarpa, R., Marconi, G., & Gilmozzi, R. 2004b, in Baryons in Dark Matter Halos, ed. R. Dettmar, P. Klein, & P. Salucci, SISSA, Proceedings of Science, 55
Scarpa, R., Marconi, G., Gilmozzi, R., & Carraro, G. 2007a, A&A, 462, L9
Scarpa, R., Marconi, G., Gilmozzi, R., & Carraro, G. 2007b, the Messenger, 128, 41
Sofue, Y., & Rubin, V. 2001, ARA&A, 39, 137
Sollima, A., Bellazzini, M., Smart, R. L., et al. 2009, MNRAS, 396, 2183
Sommariva, V., Piotto, G., Rejkuba, M., et al. 2009, A&A, 493, 947
Vanhollebeke, E., Groenewegen, M. A. T., & Girardi, L. 2009, A&A, 498, 95
Wilkinson, M. I., Kleyna, J. T., Gilmore, G. F., et al. 2006, the Messenger, 124, 25

Pages 8 to 10 are available in the electronic edition of the journal at http://www.aanda.org

Table 2. Radial velocities of stars NGC 1851.

#	ID	RA (2000)	Dec (2000)	Vel [km s^{-1}]	N	V mag
1	14729	05:13:23.70	−40:05:00.5	320.8 ± 0.7	5	18.8
2	13007	05:13:29.96	−40:11:57.2	313.6 ± 1.9	3	18.5
3	14589	05:13:29.97	−40:05:34.2	321.8 ± 1.9	5	18.7
4	15021	05:13:30.49	−40:04:12.6	312.7 ± 0.9	5	18.5
5	15277	05:13:32.52	−40:03:45.4	318.7 ± 0.5	5	18.1
6	14655	05:13:35.32	−40:05:18.4	315.2 ± 0.7	5	18.4
7	14294	05:13:35.66	−40:06:40.3	319.4 ± 0.9	5	18.2
8	14141	05:13:37.15	−40:07:18.5	328.7 ± 1.2	4	18.9
9	14831	05:13:37.43	−40:04:41.1	322.0 ± 1.4	4	18.6
10	14080	05:13:38.68	−40:07:39.5	318.5 ± 0.0	10	14.3
11	16298	05:13:40.09	−40:00:41.6	320.7 ± 0.2	5	18.2
12	16651	05:13:40.44	−39:59:26.4	318.8 ± 0.4	5	18.7
13	13707	05:13:41.25	−40:09:47.1	314.1 ± 0.3	5	18.2
14	15389	05:13:43.31	−40:03:24.7	312.6 ± 0.8	4	18.8
15	19022	05:13:46.77	−40:09:29.8	320.4 ± 0.6	5	18.4
16	19884	05:13:46.98	−40:07:28.5	312.6 ± 0.1	2	19.0
17	24548	05:13:47.44	−40:04:40.0	321.0 ± 0.4	5	18.5
18	19564	05:13:47.89	−40:08:02.6	320.0 ± 0.8	5	18.9
19	31154	05:13:48.33	−40:03:15.3	327.3 ± 0.0	10	15.5
20	19796	05:13:48.39	−40:07:37.5	323.4 ± 0.8	5	18.8
21	39698	05:13:48.46	−40:01:38.6	318.8 ± 0.3	5	18.3
22	21885	05:13:48.79	−40:05:40.3	316.9 ± 0.3	5	18.7
23	46609	05:13:48.85	−39:59:06.7	322.8 ± 1.7	4	19.0
24	30057	05:13:50.77	−40:03:27.0	322.4 ± 0.4	5	19.0
25	29934	05:13:50.87	−40:03:28.3	312.8 ± 1.2	4	19.0
26	19307	05:13:51.16	−40:08:38.4	318.3 ± 0.4	5	18.8
27	26382	05:13:51.77	−40:04:12.1	310.4 ± 0.6	5	18.7
28	21182	05:13:51.81	−40:06:05.8	316.0 ± 0.6	5	18.9
29	27495	05:13:51.85	−40:03:57.6	320.3 ± 0.4	5	18.8
30	18850	05:13:52.04	−40:10:05.1	315.5 ± 0.4	5	18.4
31	20253	05:13:52.38	−40:06:57.7	323.6 ± 1.1	5	18.7
32	27882	05:13:52.97	−40:03:52.8	319.6 ± 0.3	5	18.2
33	43446	05:13:53.03	−40:00:43.1	319.4 ± 0.0	10	14.1
34	31790	05:13:53.05	−40:03:07.7	318.1 ± 1.1	5	18.8
35	46323	05:13:53.18	−39:59:20.3	313.9 ± 1.0	5	19.0
36	19139	05:13:53.35	−40:09:05.0	322.4 ± 1.4	5	18.8
37	22073	05:13:53.53	−40:05:34.1	319.4 ± 0.5	5	18.7
38	3192	05:13:53.57	−39:55:17.9	320.4 ± 0.1	10	14.1
39	48437	05:13:53.90	−39:55:47.9	317.5 ± 0.5	5	18.4
40	21198	05:13:53.92	−40:06:05.0	312.5 ± 0.9	4	19.0
41	33397	05:13:54.09	−40:02:49.2	327.4 ± 0.5	5	18.3
42	33956	05:13:54.18	−40:02:43.6	328.6 ± 0.3	5	18.1
43	21565	05:13:54.20	−40:05:51.3	317.3 ± 1.9	3	19.0
44	28695	05:13:54.24	−40:03:42.7	320.2 ± 0.4	5	18.8
45	37483	05:13:54.47	−40:02:04.2	313.1 ± 0.3	5	18.3
46	39130	05:13:55.58	−40:01:45.1	326.6 ± 0.4	5	18.8
47	23915	05:13:55.63	−40:04:50.8	325.9 ± 0.2	5	18.2
48	45220	05:13:55.93	−40:00:00.5	322.4 ± 0.2	5	18.2
49	46912	05:13:56.62	−39:58:47.8	320.7 ± 0.3	5	18.0
50	31377	05:13:56.63	−40:03:12.4	319.6 ± 0.8	5	18.9
51	43998	05:13:56.97	−40:00:31.8	319.3 ± 0.3	5	18.4
52	41426	05:13:57.03	−40:01:15.3	317.1 ± 0.3	5	18.4
53	36571	05:13:57.16	−40:02:14.1	327.0 ± 0.7	5	19.0
54	44134	05:13:57.69	−40:00:28.7	322.5 ± 0.5	5	18.8
55	38261	05:13:57.71	−40:01:55.4	324.5 ± 0.5	5	18.7
56	30298	05:13:57.88	−40:03:24.4	323.5 ± 0.3	5	18.5
57	27236	05:13:58.13	−40:04:00.6	312.8 ± 0.5	5	18.7
58	19324	05:13:58.24	−40:08:34.7	327.6 ± 0.7	5	18.9
59	22905	05:13:58.26	−40:05:11.7	313.7 ± 0.5	5	19.0
60	19443	05:13:58.78	−40:08:19.0	312.6 ± 0.3	5	18.5
61	32453	05:13:59.00	−40:02:59.9	314.9 ± 0.2	5	18.2
62	34013	05:13:59.08	−40:02:42.8	323.4 ± 0.3	5	18.4
63	22212	05:13:59.12	−40:05:30.2	314.6 ± 0.3	5	18.5
64	35699	05:13:59.29	−40:02:24.1	311.6 ± 0.4	5	18.5
65	24570	05:13:59.47	−40:04:39.3	319.3 ± 0.4	5	18.9
66	22741	05:14:00.05	−40:05:15.8	327.6 ± 1.1	5	18.8
67	41045	05:14:00.19	−40:01:20.8	313.4 ± 0.1	5	18.3
68	47835	05:14:00.69	−39:57:20.0	323.0 ± 0.8	5	18.9
69	34266	05:14:00.72	−40:02:40.1	314.9 ± 0.3	5	18.1
70	21112	05:14:00.96	−40:06:08.1	323.6 ± 0.4	5	19.0
71	40916	05:14:01.03	−40:01:22.4	325.0 ± 0.4	5	18.2
72	33116	05:14:01.05	−40:02:52.0	324.6 ± 0.6	5	19.0
73	31177	05:14:01.24	−40:03:14.7	313.8 ± 0.6	5	18.6
74	28311	05:14:01.76	−40:03:47.2	327.5 ± 0.2	5	18.0
75	20826	05:14:02.73	−40:06:21.2	317.2 ± 0.4	3	19.0
76	47497	05:14:03.12	−39:57:57.2	319.3 ± 0.4	5	18.2
77	20350	05:14:03.17	−40:06:50.6	318.7 ± 1.3	5	18.9
78	37003	05:14:03.21	−40:02:09.3	317.3 ± 0.2	5	18.3
79	23472	05:14:03.37	−40:04:59.0	313.4 ± 0.4	5	18.1
80	21134	05:14:03.86	−40:06:07.3	320.7 ± 0.3	5	18.6
81	31131	05:14:03.86	−40:03:15.0	324.8 ± 0.5	5	18.7
82	27070	05:14:03.93	−40:04:02.7	311.8 ± 0.3	5	18.2
83	42138	05:14:04.00	−40:01:04.6	315.3 ± 0.3	5	18.5
84	19554	05:14:04.05	−40:08:03.5	316.2 ± 0.8	5	19.0
85	22153	05:14:04.07	−40:05:31.8	320.0 ± 0.6	5	18.5
86	45651	05:14:04.07	−39:59:46.4	312.3 ± 0.1	5	18.6
87	39581	05:14:04.30	−40:01:39.7	318.3 ± 0.2	5	18.0
88	42097	05:14:04.32	−40:01:05.1	325.8 ± 0.1	5	18.1
89	39271	05:14:04.65	−40:01:43.2	308.3 ± 0.4	5	18.0
90	46822	05:14:04.69	−39:58:53.4	319.2 ± 0.3	5	18.5
91	27204	05:14:04.87	−40:04:01.0	318.1 ± 1.0	5	18.9
92	22677	05:14:04.91	−40:05:17.2	324.7 ± 0.7	5	18.8
93	48120	05:14:05.03	−39:56:36.4	43.5 ± 0.3	5	18.4
94	42745	05:14:05.43	−40:00:54.7	314.6 ± 0.4	5	18.4
95	40502	05:14:05.52	−40:01:27.7	311.8 ± 0.5	5	18.5
96	28639	05:14:05.63	−40:03:43.2	308.3 ± 0.4	5	18.4
97	46458	05:14:05.97	−39:59:13.5	318.4 ± 0.3	5	18.0
98	21828	05:14:05.98	−40:05:41.9	312.4 ± 0.4	5	18.8
99	21165	05:14:06.00	−40:06:06.3	328.7 ± 0.3	5	18.9
100	19309	05:14:06.94	−40:08:37.8	317.8 ± 0.8	5	19.0
101	45709	05:14:07.16	−39:59:44.3	330.2 ± 0.2	5	18.8
102	26167	05:14:07.35	−40:04:14.7	319.4 ± 0.2	5	18.5
103	46644	05:14:07.44	−39:59:04.4	316.8 ± 1.4	5	19.0
104	45848	05:14:07.50	−39:59:39.3	318.1 ± 0.5	5	18.5
105	28825	05:14:07.59	−40:03:40.6	332.1 ± 0.4	5	18.4
106	38957	05:14:07.79	−40:01:47.2	329.7 ± 0.2	5	18.3
107	19805	05:14:08.17	−40:07:36.0	322.5 ± 0.4	5	18.1
108	22255	05:14:08.57	−40:05:28.5	320.5 ± 0.5	5	18.9
109	19200	05:14:08.81	−40:08:54.8	314.8 ± 1.2	4	18.9
110	20851	05:14:08.92	−40:06:19.5	318.2 ± 0.4	5	18.7
111	46908	05:14:08.94	−39:58:47.9	316.5 ± 0.2	5	18.3
112	46096	05:14:08.94	−39:59:30.1	314.9 ± 0.5	5	19.0
113	44889	05:14:08.96	−40:00:09.4	320.5 ± 0.4	5	18.1
114	46433	05:14:09.16	−39:59:14.5	315.2 ± 1.0	4	19.0
115	18656	05:14:09.71	−40:10:44.6	315.6 ± 1.0	5	18.4
116	40705	05:14:09.84	−40:01:24.8	330.4 ± 0.1	5	18.3
117	39847	05:14:09.86	−40:01:36.2	313.9 ± 0.0	5	13.9
118	39006	05:14:10.11	−40:01:46.4	324.1 ± 0.3	5	18.2
119	29582	05:14:10.23	−40:03:31.7	326.0 ± 1.1	5	18.2
120	41432	05:14:10.73	−40:01:14.9	321.4 ± 0.5	5	18.8
121	48457	05:14:11.04	−39:55:43.9	317.3 ± 1.1	5	19.0
122	41502	05:14:11.23	−40:01:13.7	313.6 ± 0.4	5	18.8
123	20559	05:14:11.34	−40:06:37.4	315.7 ± 0.7	3	19.0
124	38347	05:14:11.90	−40:01:53.9	328.8 ± 0.5	5	18.9
125	43953	05:14:12.04	−40:00:32.3	319.7 ± 0.6	5	19.0
126	38826	05:14:12.29	−40:01:48.7	327.3 ± 0.8	5	18.7
127	47224	05:14:12.29	−39:58:24.7	321.4 ± 0.1	5	18.8
128	23057	05:14:12.35	−40:05:07.5	319.5 ± 0.4	5	18.5
129	25840	05:14:12.46	−40:04:19.1	316.9 ± 0.4	5	18.9
130	45531	05:14:12.94	−39:59:50.3	328.1 ± 1.0	5	19.0
131	22278	05:14:13.00	−40:05:27.7	319.8 ± 0.6	5	18.7
132	28104	05:14:13.10	−40:03:49.6	309.0 ± 0.2	5	19.0
133	40619	05:14:13.54	−40:01:25.7	314.4 ± 0.1	5	18.3
134	21810	05:14:13.86	−40:05:42.1	318.0 ± 0.3	5	18.7
135	46033	05:14:14.28	−39:59:32.3	314.9 ± 0.8	4	19.0
136	41419	05:14:14.72	−40:01:14.9	326.9 ± 0.5	5	19.0
137	18150	05:14:14.78	−40:11:38.9	320.4 ± 0.6	5	18.0
138	42970	05:14:15.08	−40:00:50.7	317.4 ± 0.1	5	18.2
139	26485	05:14:15.08	−40:04:09.9	320.2 ± 0.6	5	19.0
140	39875	05:14:15.17	−40:01:35.7	323.3 ± 0.5	4	18.5
141	25964	05:14:15.48	−40:04:17.2	322.5 ± 0.6	5	18.9
142	27421	05:14:15.57	−40:03:57.8	326.2 ± 0.4	5	18.6
143	21484	05:14:15.80	−40:05:53.4	324.1 ± 1.1	4	19.0
144	46479	05:14:15.84	−39:59:12.1	326.4 ± 0.3	5	18.5
145	17879	05:14:16.25	−40:11:57.1	318.1 ± 0.8	4	18.9
146	42908	05:14:16.29	−40:00:51.8	318.9 ± 0.2	5	18.2
147	25605	05:14:16.59	−40:04:22.3	323.9 ± 0.6	5	19.0
148	43709	05:14:16.75	−40:00:37.0	324.6 ± 0.9	5	19.0
149	40153	05:14:16.76	−40:01:32.0	324.6 ± 0.4	5	19.0
150	33925	05:14:16.77	−40:02:43.2	318.8 ± 0.3	5	18.1
151	44016	05:14:16.92	−40:00:30.7	323.2 ± 0.9	4	19.0
152	26933	05:14:16.96	−40:04:03.9	315.9 ± 0.4	5	18.8
153	42256	05:14:17.06	−40:01:02.2	329.0 ± 1.2	5	18.9
154	46284	05:14:17.90	−39:59:21.3	322.0 ± 0.4	5	18.4
155	31495	05:14:17.91	−40:03:10.4	320.4 ± 0.3	4	19.0
156	45371	05:14:17.99	−39:59:55.4	315.3 ± 0.3	5	18.0
157	37497	05:14:18.08	−40:02:03.2	316.1 ± 0.3	5	18.3
158	26282	05:14:18.74	−40:04:12.7	321.1 ± 0.4	5	18.7
159	29424	05:14:19.08	−40:03:33.2	321.7 ± 0.1	5	18.2
160	42103	05:14:19.55	−40:01:04.5	325.4 ± 0.2	5	18.9
161	46497	05:14:20.25	−39:59:11.0	320.0 ± 0.3	5	18.4
162	19441	05:14:20.71	−40:08:18.5	321.7 ± 0.5	5	18.6
163	35357	05:14:20.72	−40:02:27.4	324.4 ± 0.2	5	18.1
164	40709	05:14:20.83	−40:01:24.3	320.7 ± 0.6	5	18.9

Table 2. continued.

#	ID	RA (2000)	Dec (2000)	Vel [km s^{-1}]	N	V mag
165	20506	05:14:20.91	−40:06:39.8	325.5 ± 0.4	5	18.6
166	30021	05:14:21.10	−40:03:26.5	319.3 ± 0.1	4	18.1
167	45097	05:14:21.40	−40:00:02.9	320.7 ± 0.4	5	18.2
168	19664	05:14:21.70	−40:07:49.9	320.5 ± 0.6	5	18.7
169	34410	05:14:22.03	−40:02:37.7	313.2 ± 0.2	5	18.9
170	44618	05:14:22.11	−40:00:16.4	321.8 ± 0.1	5	18.2
171	24751	05:14:22.18	−40:04:35.3	323.0 ± 0.2	5	18.1
172	27965	05:14:22.43	−40:03:51.0	322.3 ± 0.9	5	18.8
173	46681	05:14:22.56	−39:59:01.7	316.0 ± 0.3	5	18.7
174	28310	05:14:22.91	−40:03:46.4	325.6 ± 0.3	5	18.6
175	22954	05:14:23.07	−40:05:09.8	315.8 ± 0.5	5	18.6
176	40476	05:14:23.85	−40:01:27.4	326.3 ± 0.7	5	18.9
177	3799	05:14:24.22	−39:52:30.3	321.8 ± 0.8	5	18.9
178	3717	05:14:24.44	−39:53:12.2	320.7 ± 0.7	5	18.5
179	24263	05:14:24.82	−40:04:43.8	316.5 ± 0.4	5	18.4
180	20919	05:14:25.10	−40:06:15.2	321.1 ± 0.1	5	18.8
181	24840	05:14:25.16	−40:04:33.5	320.0 ± 0.4	5	18.8
182	41815	05:14:25.32	−40:01:08.6	317.5 ± 0.9	5	18.9
183	32903	05:14:25.97	−40:02:53.8	319.7 ± 0.1	10	13.8
184	22338	05:14:26.21	−40:05:25.6	322.8 ± 0.4	5	18.3
185	45391	05:14:26.72	−39:59:54.5	310.0 ± 0.5	5	18.5
186	3498	05:14:27.29	−39:54:24.5	322.6 ± 0.4	5	18.2
187	34212	05:14:27.64	−40:02:39.6	328.5 ± 0.5	5	18.2
188	54310	05:14:32.11	−39:57:12.7	90.2 ± 0.2	5	18.2
189	53852	05:14:32.13	−39:58:46.3	326.1 ± 0.5	5	18.8
190	49277	05:14:33.22	−40:11:13.8	319.4 ± 0.5	5	18.6
191	52750	05:14:34.75	−40:01:31.5	322.9 ± 0.6	4	18.9
192	52972	05:14:34.88	−40:00:58.6	323.0 ± 0.4	5	18.8
193	52569	05:14:36.07	−40:01:54.7	326.6 ± 0.5	5	18.9
194	51626	05:14:36.81	−40:03:59.1	322.2 ± 1.5	5	18.8
195	50507	05:14:37.48	−40:07:04.2	316.1 ± 0.3	5	18.3
196	50690	05:14:45.87	−40:06:25.4	56.7 ± 0.2	3	19.0
197	52758	05:14:48.74	−40:01:29.5	318.1 ± 0.6	3	19.0
198	51770	05:14:56.62	−40:03:37.7	318.7 ± 0.5	5	18.4
199	52120	05:15:04.47	−40:02:51.8	80.8 ± 0.8	4	18.6

Table 3. Radial velocities of stars in NGC 1904.

#	ID	RA (2000)	Dec (2000)	Vel [km s^{-1}]	N	V mag
1	1179	05:23:29.73	−24:30:26.4	35.3 ± 0.1	10	17.5
2	1443	05:23:30.75	−24:33:32.3	200.0 ± 0.8	5	17.9
3	2177	05:23:32.06	−24:27:12.5	33.5 ± 1.2	4	18.6
4	2392	05:23:41.47	−24:30:35.7	206.8 ± 0.7	5	18.8
5	2678	05:23:42.48	−24:29:01.3	203.1 ± 1.1	4	19.0
6	1370	05:23:43.53	−24:32:43.7	44.6 ± 2.8	5	17.7
7	2747	05:23:44.08	−24:29:32.9	204.7 ± 1.2	3	19.0
8	2609	05:23:44.11	−24:24:29.2	100.9 ± 0.7	4	18.3
9	1881	05:23:44.62	−24:36:41.3	203.3 ± 0.5	5	18.4
10	1930	05:23:44.72	−24:30:35.0	206.1 ± 0.3	5	18.4
11	2215	05:23:45.15	−24:34:52.6	44.6 ± 0.1	5	18.5
12	2708	05:23:45.66	−24:30:07.1	203.8 ± 0.5	3	19.1
13	2057	05:23:48.72	−24:31:30.4	204.5 ± 0.4	5	18.6
14	1569	05:23:48.78	−24:32:19.4	204.0 ± 0.3	5	18.1
15	1727	05:23:51.26	−24:31:09.9	206.5 ± 0.2	5	18.3
16	1319	05:23:51.58	−24:31:50.7	206.5 ± 0.1	5	17.7
17	1894	05:23:52.45	−24:31:36.2	209.3 ± 0.2	5	18.4
18	2158	05:23:53.39	−24:31:29.7	203.9 ± 0.5	3	18.6
19	1954	05:23:56.37	−24:30:19.0	208.0 ± 0.3	5	18.4
20	1815	05:23:56.56	−24:29:52.9	208.6 ± 0.3	5	18.3
21	2837	05:23:56.58	−24:30:37.3	207.9 ± 1.0	5	19.1
22	1484	05:23:56.70	−24:33:01.1	209.9 ± 0.2	5	17.9
23	1570	05:23:57.08	−24:29:26.3	207.9 ± 0.2	5	18.0
24	1583	05:23:57.64	−24:29:58.1	208.2 ± 0.3	5	18.0
25	1047	05:23:58.27	−24:33:40.8	200.7 ± 0.1	5	17.3
26	1857	05:23:58.38	−24:31:22.9	206.8 ± 0.3	5	18.4
27	1818	05:23:58.99	−24:29:14.6	207.3 ± 0.2	5	18.3
28	1302	05:23:59.33	−24:29:44.3	208.5 ± 0.1	5	17.6
29	2108	05:23:59.58	−24:35:05.6	206.7 ± 0.7	5	18.5
30	1275	05:23:59.84	−24:31:33.5	206.5 ± 0.1	5	17.6
31	1407	05:24:00.20	−24:30:29.9	206.3 ± 0.2	5	17.8
32	1515	05:24:00.29	−24:30:36.5	206.5 ± 0.4	5	18.0
33	2105	05:24:00.40	−24:34:38.1	204.1 ± 0.4	5	18.5
34	2568	05:24:00.95	−24:31:26.1	206.2 ± 1.7	5	19.0
35	2580	05:24:01.06	−24:29:31.6	206.7 ± 1.8	5	19.0
36	2561	05:24:01.09	−24:29:58.7	207.8 ± 0.5	5	18.8
37	1286	05:24:01.19	−24:29:01.8	210.9 ± 0.3	5	17.7
38	2820	05:24:01.83	−24:30:03.8	204.2 ± 1.0	5	19.0
39	2616	05:24:02.49	−24:32:59.8	199.6 ± 0.8	5	18.9
40	1467	05:24:02.58	−24:31:30.6	202.9 ± 0.2	5	17.9
41	1175	05:24:03.30	−24:32:28.9	202.0 ± 0.1	5	17.5
42	2748	05:24:03.53	−24:27:23.9	208.8 ± 0.6	4	19.1
43	2042	05:24:04.19	−24:30:45.6	209.4 ± 0.3	5	18.5
44	2488	05:24:04.35	−24:30:29.0	210.4 ± 0.5	5	18.8
45	949	05:24:04.44	−24:32:23.0	206.3 ± 0.1	10	17.5
46	1362	05:24:04.46	−24:29:01.8	203.7 ± 0.3	5	17.8
47	1028	05:24:04.66	−24:31:24.1	200.9 ± 0.2	5	17.2
48	2614	05:24:05.08	−24:24:45.6	207.8 ± 0.1	3	19.0
49	1525	05:24:05.43	−24:29:55.2	213.6 ± 0.2	5	18.0
50	1306	05:24:05.52	−24:30:06.7	202.2 ± 0.1	5	17.7
51	2686	05:24:05.54	−24:31:53.1	209.1 ± 0.3	5	18.9
52	2462	05:24:05.61	−24:26:58.5	207.3 ± 0.6	5	18.8
53	1916	05:24:06.00	−24:32:25.6	206.9 ± 0.4	5	18.6
54	1311	05:24:06.24	−24:35:01.5	204.2 ± 0.2	5	17.7
55	2476	05:24:06.42	−24:29:53.5	203.2 ± 0.6	5	19.0
56	2554	05:24:06.44	−24:30:33.0	208.8 ± 0.5	5	19.1
57	1322	05:24:06.47	−24:31:48.0	208.8 ± 0.3	5	17.8
58	1099	05:24:06.65	−24:33:11.2	208.2 ± 0.3	5	17.3
59	1080	05:24:07.01	−24:31:52.0	206.9 ± 0.1	5	17.2
60	1474	05:24:07.34	−24:37:58.0	205.4 ± 0.4	5	17.9
61	2294	05:24:07.39	−24:30:51.3	209.9 ± 0.4	5	18.9
62	2688	05:24:07.63	−24:27:18.0	205.8 ± 1.0	5	19.0
63	1408	05:24:07.73	−24:25:13.3	19.0 ± 0.1	5	17.4
64	1222	05:24:07.84	−24:28:07.7	205.4 ± 0.2	5	17.6
65	1388	05:24:07.84	−24:32:48.7	202.4 ± 0.2	5	17.8
66	2302	05:24:07.92	−24:30:42.5	208.7 ± 0.4	5	18.7
67	1258	05:24:07.93	−24:32:54.8	197.1 ± 0.2	5	17.6
68	999	05:24:08.04	−24:31:21.1	212.6 ± 0.2	5	17.1
69	1479	05:24:08.37	−24:30:17.8	211.3 ± 0.3	5	17.9
70	1464	05:24:08.44	−24:35:37.2	208.9 ± 0.2	5	17.9
71	1241	05:24:08.54	−24:31:58.6	209.7 ± 0.1	5	17.7
72	1375	05:24:08.64	−24:32:20.7	202.1 ± 0.2	5	17.8
73	1536	05:24:08.67	−24:26:25.8	207.4 ± 0.2	5	18.0
74	1270	05:24:09.12	−24:32:33.8	204.3 ± 0.2	5	17.7
75	1048	05:24:09.16	−24:28:46.9	205.7 ± 0.2	5	17.2
76	2086	05:24:09.16	−24:35:02.1	207.7 ± 0.2	5	18.5
77	2296	05:24:09.32	−24:30:38.7	200.5 ± 1.1	5	19.1
78	1663	05:24:09.38	−24:26:01.4	209.3 ± 0.4	5	18.2
79	1435	05:24:09.42	−24:23:11.6	204.4 ± 0.4	5	17.9
80	1628	05:24:09.44	−24:36:34.5	205.6 ± 0.2	5	18.1

Table 3. continued.

#	ID	RA (2000)	Dec (2000)	Vel [km s^{-1}]	N	V mag
81	1239	05:24:09.50	−24:32:21.3	203.1 ± 0.1	5	17.6
82	1759	05:24:09.52	−24:27:56.1	204.6 ± 0.5	5	18.2
83	1503	05:24:09.53	−24:32:56.7	205.9 ± 0.2	5	17.9
84	1372	05:24:10.22	−24:29:07.5	211.8 ± 0.2	5	17.8
85	1238	05:24:10.65	−24:33:48.6	206.9 ± 0.2	5	17.5
86	2569	05:24:10.72	−24:25:58.8	206.6 ± 1.2	4	18.9
87	1505	05:24:10.77	−24:34:13.9	203.0 ± 0.4	5	17.9
88	1482	05:24:11.40	−24:33:24.7	205.1 ± 0.3	5	17.9
89	1609	05:24:11.42	−24:29:55.2	207.8 ± 0.3	5	18.1
90	2911	05:24:11.48	−24:30:11.0	205.2 ± 0.5	5	19.1
91	1007	05:24:11.52	−24:32:22.2	204.4 ± 0.1	5	17.1
92	1779	05:24:12.02	−24:33:56.3	205.5 ± 0.2	5	18.2
93	1353	05:24:12.03	−24:34:49.4	205.0 ± 0.3	5	17.7
94	2485	05:24:12.05	−24:29:28.6	206.9 ± 1.2	4	19.1
95	1428	05:24:12.21	−24:30:21.5	209.5 ± 0.1	5	17.9
96	1194	05:24:12.33	−24:31:21.8	205.1 ± 0.3	5	17.5
97	970	05:24:12.34	−24:30:33.0	201.5 ± 0.4	5	17.1
98	1298	05:24:12.45	−24:29:39.0	205.7 ± 0.2	5	17.7
99	2027	05:24:12.54	−24:28:44.4	210.0 ± 0.4	5	18.5
100	1303	05:24:12.57	−24:32:24.3	199.7 ± 0.2	5	17.8
101	1109	05:24:12.88	−24:31:06.6	201.2 ± 0.1	5	17.3
102	1411	05:24:13.18	−24:27:04.8	207.5 ± 0.3	5	17.8
103	1540	05:24:13.19	−24:33:22.3	204.0 ± 0.2	5	17.9
104	1371	05:24:13.90	−24:32:34.5	202.8 ± 0.2	5	17.7
105	968	05:24:14.11	−24:31:49.6	202.1 ± 0.2	5	17.0
106	1199	05:24:14.11	−24:32:38.7	211.9 ± 0.1	5	17.6
107	1683	05:24:14.18	−24:30:43.8	207.7 ± 0.2	5	18.1
108	1263	05:24:14.20	−24:32:47.9	204.6 ± 0.2	5	17.7
109	2009	05:24:14.26	−24:27:19.7	207.4 ± 0.4	5	18.6
110	1971	05:24:14.99	−24:32:15.6	203.1 ± 0.4	5	18.5
111	1442	05:24:15.06	−24:30:01.7	210.3 ± 0.4	5	17.9
112	1888	05:24:15.09	−24:32:53.8	197.9 ± 0.2	5	18.4
113	1577	05:24:15.28	−24:31:56.6	207.2 ± 0.2	5	18.0
114	1250	05:24:15.41	−24:32:35.2	206.8 ± 0.1	5	17.6
115	2704	05:24:15.63	−24:28:37.6	202.7 ± 0.3	4	19.0
116	1834	05:24:15.78	−24:30:37.7	206.7 ± 0.4	5	18.4
117	1555	05:24:15.81	−24:30:52.6	205.0 ± 0.2	5	18.1
118	1427	05:24:15.94	−24:32:20.2	200.9 ± 0.1	5	17.9
119	1060	05:24:16.03	−24:30:37.5	211.6 ± 0.1	5	17.2
120	1341	05:24:16.35	−24:29:37.3	202.2 ± 0.2	5	17.7
121	1802	05:24:16.57	−24:35:55.5	204.7 ± 0.3	5	18.2
122	2400	05:24:16.70	−24:32:17.1	204.3 ± 0.7	5	19.1
123	1932	05:24:16.71	−24:33:00.5	209.5 ± 0.3	5	18.4
124	1522	05:24:17.09	−24:27:57.3	206.8 ± 0.4	5	18.0
125	1715	05:24:17.15	−24:32:29.4	210.4 ± 0.3	5	18.2
126	2150	05:24:17.33	−24:28:50.7	204.5 ± 0.6	5	18.6
127	1212	05:24:17.37	−24:30:54.2	202.3 ± 0.2	5	17.5
128	1208	05:24:17.42	−24:29:38.5	208.1 ± 0.1	5	17.5
129	1909	05:24:17.74	−24:31:09.1	209.5 ± 0.7	5	18.4
130	1596	05:24:17.83	−24:32:08.1	209.8 ± 0.3	5	18.0
131	1498	05:24:17.98	−24:38:23.9	204.3 ± 0.2	5	17.9
132	1058	05:24:18.60	−24:24:55.8	202.5 ± 0.2	5	17.2
133	2551	05:24:18.74	−24:28:30.8	205.1 ± 1.4	5	19.0
134	1762	05:24:19.31	−24:27:53.6	210.4 ± 0.5	5	18.3
135	1145	05:24:19.67	−24:31:06.3	209.1 ± 0.1	5	17.4
136	1597	05:24:19.93	−24:32:46.0	203.3 ± 0.4	5	18.1
137	1304	05:24:20.17	−24:34:08.4	205.5 ± 0.1	5	17.6
138	1015	05:24:20.33	−24:33:14.7	202.6 ± 0.1	10	17.5
139	2539	05:24:20.36	−24:25:20.6	35.4 ± 0.2	5	18.3
140	1728	05:24:20.41	−24:26:40.8	204.9 ± 0.3	5	18.2
141	1820	05:24:20.49	−24:28:54.4	203.2 ± 0.3	5	18.3
142	2336	05:24:21.36	−24:29:37.3	207.0 ± 0.5	5	18.8
143	2394	05:24:21.57	−24:29:12.4	208.1 ± 0.8	5	18.8
144	2393	05:24:21.60	−24:32:16.2	206.6 ± 0.6	5	18.7
145	1422	05:24:22.04	−24:31:01.3	208.8 ± 0.4	5	17.8
146	1069	05:24:22.39	−24:31:51.3	204.9 ± 0.1	5	17.2
147	2703	05:24:22.68	−24:30:55.1	209.9 ± 0.6	5	19.0
148	1810	05:24:22.81	−24:33:43.7	211.4 ± 0.2	5	18.2
149	1858	05:24:23.14	−24:31:30.7	204.1 ± 0.7	5	18.3
150	1123	05:24:23.16	−24:25:56.0	205.6 ± 0.3	5	17.4
151	1804	05:24:23.55	−24:34:18.9	208.1 ± 0.2	5	18.2
152	2574	05:24:23.78	−24:25:49.1	208.6 ± 1.1	5	19.0
153	2048	05:24:24.04	−24:32:13.5	205.5 ± 0.4	5	18.5
154	1749	05:24:24.68	−24:31:40.4	201.9 ± 0.2	5	18.2
155	1890	05:24:25.61	−24:35:15.9	207.0 ± 0.3	5	18.3
156	2606	05:24:25.79	−24:30:39.1	202.2 ± 1.1	5	19.1
157	2033	05:24:26.47	−24:23:14.5	11.1 ± 0.2	5	18.1
158	2345	05:24:26.75	−24:32:23.0	207.8 ± 0.7	5	18.7
159	1973	05:24:27.93	−24:29:26.5	209.7 ± 0.5	5	18.5
160	1373	05:24:28.38	−24:25:16.0	38.1 ± 0.3	5	17.2

Table 3. continued.

#	ID	RA (2000)	Dec (2000)	Vel [km s^{-1}]	N	V mag
161	1410	05:24:28.65	−24:31:43.6	204.3 ± 0.3	5	17.9
162	2597	05:24:28.69	−24:28:05.9	208.0 ± 0.9	5	19.0
163	2354	05:24:28.78	−24:22:57.7	76.9 ± 1.7	4	18.3
164	1939	05:24:29.02	−24:37:35.7	206.0 ± 0.5	5	18.4
165	2434	05:24:29.18	−24:30:42.4	204.5 ± 0.4	5	18.7
166	2367	05:24:29.51	−24:27:36.1	202.5 ± 1.1	5	18.8
167	1151	05:24:30.97	−24:31:41.4	−21.5 ± 0.1	5	17.2
168	2843	05:24:31.06	−24:30:45.9	207.2 ± 1.3	3	19.1
169	1439	05:24:38.78	−24:37:15.9	40.5 ± 0.2	5	17.9
170	2115	05:24:41.18	−24:33:52.3	209.1 ± 0.7	5	18.6
171	1190	05:24:41.26	−24:33:41.2	207.6 ± 0.2	5	17.5
172	1702	05:24:46.57	−24:34:31.5	205.4 ± 0.6	4	18.2
173	1162	05:24:53.79	−24:36:01.8	80.4 ± 0.1	10	17.5